Journal of **RAMAN SPECTROSCOPY**

High-resolution narrowband CARS spectroscopy in the spectral fingerprint region

P. F. Chimento,[a†] **M. Jurna,**[a] **H. S. P. Bouwmans,**[a] **E. T. Garbacik,**[a] **L. Hartsuiker,**[b] **C. Otto,**[b] **J. L. Herek**[a] **and H. L. Offerhaus**[a*]

Coherent anti-Stokes Raman scattering (CARS) spectroscopy is an important technique for spectroscopy and chemically selective microscopy, but wider implementation requires dedicated versatile tunable sources. We describe an optical parametric oscillator (OPO) based on a magnesium oxide-doped periodically poled lithium niobate crystal, with a novel variable output coupler, used as a tunable coherent light source. The OPO's signal wavelength ranges from 880 to 1040 nm and its idler wavelength from 1090 to 1350 nm.

We use this OPO to demonstrate high-resolution narrowband CARS spectroscopy on bulk polystyrene from 900 to 3600 cm^{-1}, covering a large part of the molecular fingerprint region. Recording vibrational spectra using narrowband CARS spectroscopy has several advantages over spontaneous Raman spectroscopy, which we discuss. We isolate the resonant part of the CARS spectrum and compare it to the spontaneous Raman spectrum of polystyrene using the maximum entropy method of phase retrieval; we find them to be in extremely good agreement. Copyright © 2009 John Wiley & Sons, Ltd.

Keywords: coherent anti-Stokes Raman scattering (CARS); CARS spectroscopy; optical parametric oscillator; maximum entropy method

Introduction

Coherent anti-Stokes Raman scattering (CARS) is a widely proven technique for chemically selective microscopy based on the vibrational spectrum of a molecule.[1] However, CARS is also a useful tool for vibrational spectroscopy, an area that is traditionally covered by spontaneous Raman. Figure 1 shows an energy diagram of CARS. Two waves, the pump wave at frequency ω_p and the Stokes wave at frequency ω_s, drive an interaction field in a sample at the Raman shift frequency $\Omega = \omega_p - \omega_s$, which interacts with the probe wave at frequency ω_{pr} to produce the anti-Stokes wave at frequency $\omega_{as} = \omega_p - \omega_s + \omega_{pr}$. Typically, degenerate CARS is used, in which the pump and probe waves are the same, so that $\omega_{as} = 2\omega_p - \omega_s$.

CARS can be used to probe the vibrational spectrum of a sample, since the CARS process is enhanced when the pump and Stokes' interaction frequency $\omega_p - \omega_s$ coincides with a molecular vibration. CARS is a coherent process, and the CARS signal is not scattered in all directions, as in spontaneous Raman, but instead emerges in a coherent beam, facilitating detection with high collection efficiency. As the signal from all the coherently oscillating dipoles adds in phase, the output intensity is quadratic in the number of dipoles (the concentration) rather than linear as in Raman scattering. Consequently, CARS signals can be detected much more easily and faster than Raman scattered signals but reconstruction of a mixture is more involved. Narrowband CARS spectroscopy can only probe one molecular vibration at a time, whereas typical Raman spectroscopy gathers information on the sample's entire spectrum at once. Addressing only one vibration is an advantage for microscopy, but a disadvantage for spectroscopy and compositional analysis. The combination of narrowband CARS and a rapidly tunable coherent light source allows easy detection of the CARS signal with a single photodetector.[2]

This paper describes the design and operation of an optical parametric oscillator (OPO) as a tunable light source for narrowband CARS spectroscopy, and experimental spectroscopy results are demonstrated over a wide range of Raman shifts extending from 900 to 3600 cm^{-1}.

Resonant and Nonresonant CARS

Under conditions of perfect phase matching, the CARS output is a function of the third-order nonlinear susceptibility tensor $\chi^{(3)}$ of the material. Hereafter, we will use $\chi^{(3)}$ to denote only the relevant component of the tensor. The intensity I_{as} of the anti-Stokes beam in a degenerate CARS process is then given by:

$$I_{as} \propto \omega_{as}^2 |\chi^{(3)}|^2 I_p^2 I_s D^2, \tag{1}$$

where ω_{as} is the anti-Stokes frequency, I_p and I_s are the intensities of the pump/probe and Stokes beams, respectively, and D is the interaction length given by the sample thickness or focal length. The vibrational resonances can be modelled as driven oscillators. The CARS susceptibility is composed of a nonresonant contribution, and a resonant contribution proportional to the

---

* Correspondence to: H. L. Offerhaus, Optical Sciences Group, Department of Science and Technology, MESA$^+$ Institute for Nanotechnology, University of Twente, 7500 AE Enschede, The Netherlands. E-mail: h.l.offerhaus@utwente.nl

† Current address: Huygens Laboratory, Leiden University, P. O. Box 9504, 2300 RA Leiden, The Netherlands.

a Optical Sciences Group, Department of Science and Technology, MESA$^+$ Institute for Nanotechnology, University of Twente, 7500 AE Enschede, The Netherlands

b Biophysical Engineering Group, Institute for Biomedical Technology, and MESA$^+$ Institute for Nanotechnology, University of Twente, 7500 AE Enschede, The Netherlands
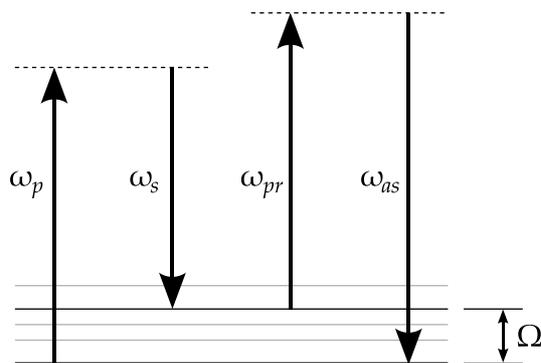
Figure 1. Energy diagram of CARS, where the interaction frequency $\omega_p - \omega_s$ is tuned to a molecular vibration Ω, which is probed by the probe frequency ω_{pr}. The dotted lines represent states that are not eigenstates of the molecule.

vibrational response[3]:

$$\chi^{(3)}(\omega) \propto \chi_{NR}^{(3)} + \sum_R \frac{A_R}{\Omega_R^2 - \omega^2 - 2i\omega\Gamma_R}, \qquad (2)$$

where A_R is the strength of Raman resonance R, Ω_R the frequency, and Γ_R the full width at half maximum. The $\chi_{NR}^{(3)}$ term is the nonresonant contribution which includes the contributions for two-photon electronic pathways. Electronic resonances are avoided through the use of near-infrared wavelengths.[4]

The intensity of spontaneous Raman scattering is proportional to the imaginary part of Eqn (2)[5]:

$$I_{Raman}(\omega) \propto -Im[\chi^{(3)}(\omega)] = \sum_R \frac{2\omega A_R \Gamma_R}{(\Omega_R^2 - \omega^2)^2 + 4\omega^2 \Gamma_R^2}. \qquad (3)$$

The CARS intensity is proportional to $|\chi^{(3)}|^2$, as shown in Eqn (1). Squaring Eqn (2) yields a constant nonresonant term, a Lorentzian resonant term, and a mixing term,[6] which causes the local maximum of the CARS lineshape to appear at a lower wavenumber than its corresponding Raman peak. In the presence of multiple components, all the components interfere and the shift is determined by the mixing of all the complex amplitudes. In the spectral fingerprint region of molecules, with many resonances close together, the mixing quickly becomes difficult to unravel. This is further complicated by the nonresonant and resonant responses also depending on the pulse spectral width of the excitation light: at spectral widths larger than the spectral width of the Raman resonance, the resonant response is saturated, whereas the total nonresonant response over all frequencies depends quadratically on the spectral width.[7] The spectral widths of the excitation pulses also govern the CARS spectral resolution, which Cheng *et al.*[7] estimate to be:

$$\Delta\tilde{\nu}_{CARS} = \sqrt{\Delta\tilde{\nu}_{pump}^2 + \Delta\tilde{\nu}_{Stokes}^2}, \qquad (4)$$

where $\Delta\tilde{\nu}$ is the spectral full width at half maximum. These dependences on the spectral widths prevent the pure CARS spectrum from being interpreted quantitatively. In order to be useful for molecular identification using the well-known Raman peaks, the resonant CARS signal must be extracted from the total CARS signal.

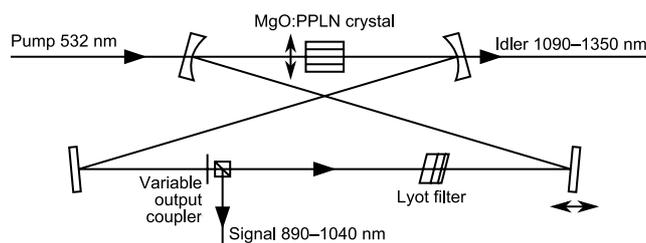Heterodyne interferometric detection exploits the phase difference between the resonant and nonresonant contributions: By measuring the phase difference between the anti-Stokes wave and the pump/probe and Stokes waves, the imaginary part of $\chi^{(3)}$ can be isolated and compared directly to the Raman spectrum.[8,9]

Another method of determining the phase difference and thus the Raman spectrum is the maximum entropy method.[10] It can be used to extract the phase information mathematically from the CARS spectrum without *a priori* knowledge of the Raman spectrum but it requires a sufficiently broad portion of the CARS spectrum, including areas containing no resonances, to effectively determine the phase. Here, we apply it for the first time to narrowband CARS spectroscopy. In situations where detector noise is not a concern and a large portion of the spectrum is to be measured, the maximum entropy method is an attractive alternative to heterodyne detection.

Figure 2. Schematic of the OPO setup. The OPO consists of a signal resonant ring cavity, the length of which is adjustable by moving one of the flat mirrors. The MgO:PPLN crystal can be moved to select the appropriate poling domain. The cavity also contains a Lyot filter in order to reduce the signal bandwidth and a variable output coupler.

Experimental

Figure 2 shows a sketch of the experimental setup. A mode-locked picosecond Nd:YVO$_4$ laser (Coherent Paladin) was modified to produce frequency-doubled green light at 532 nm, and fitted with an extra output port for the fundamental 1064 nm wavelength. The laser's repetition rate was 80 MHz. The 532 nm second-harmonic beam, attenuated to 330 mW, was used to pump the OPO. The OPO was also tested with a second pump laser (Spectra Physics Vanguard) with the same output frequencies and repetition rate.

The OPO is based on a 5 mol% magnesium oxide-doped periodically poled lithium niobate (MgO:PPLN) crystal (HC Photonics Corp.) It is synchronously pumped and has a standard ring cavity which is singly resonant for the signal wave.[11] This singly resonant cavity allows for the possibility of using it for heterodyne interferometric detection in the future. The cavity is formed by two concave mirrors and two plane mirrors (CVI Laser Optics LLC). The concave mirrors' radii of curvature are 257.5 mm. The cavity mirrors are highly reflective in the range of 890–1040 nm. The MgO:PPLN crystal has six poling domains, four of which are used in these experiments: 6.80, 6.85, 6.90 and 6.95 μm. The crystal's end faces have a coating which has high transmission at the pump, signal and idler wavelengths. The interaction in the crystal is type IV ($e \rightarrow e + e$), and the required pump polarisation is perpendicular to the plane of Fig.2. The cavity length is equal to the spatial separation between two pulses from the laser, and adjustable by moving one of the cavity mirrors, mounted on a translation stage. The cavity also incorporates a Lyot filter in order to reduce the signal bandwidth.

The MgO:PPLN crystal is mounted in an oven and its temperature can be tuned between ambient and 170 °C. The

oven is mounted on a translation stage allowing selection of the poling domain, which is used for coarse wavelength tuning.

Another feature of the OPO is the variable output coupler built into the cavity. Any desired amount of signal light can be coupled out of the cavity by the variable output coupler, consisting of a half-wave plate and a polarising beam cube to remove the *o*-polarised component. The OPO's oscillation threshold is influenced depending on the fraction of the signal light removed from the cavity.

The signal output from the OPO (typically 30 mW) is used as the pump/probe input to the CARS process. The 1064 nm fundamental of the laser (100 mW) and the idler output from the OPO (typically 30 mW) can both be used as the Stokes input, referred to as 'fundamental mode' and 'idler mode', respectively. In both cases, the choice of infrared excitation wavelengths avoids two-photon resonances.[4]

The pump/probe and Stokes are combined on a dichroic mirror, and focused into the sample using a 0.60 NA microscope objective. This tight focusing relaxes the phase matching condition.[12,13] The light is collected using a 0.40 NA objective with an extra long working distance, allowing extra room for focusing in large samples. The anti-Stokes light is separated from the remaining pump/probe and Stokes light, using a set of interference filters, and detected using a photomultiplier tube (Hamamatsu H6780-20).

To better detect the weak anti-Stokes signal, and reduce 1/*f* noise, the photomultiplier tube's output signal is processed by a software lock-in amplifier.[14] The reference signal is obtained by modulating the Stokes beam with an optical chopper at 490 Hz.

The CARS spectra were recorded using a custom-built data acquisition program written in LabVIEW. A small fraction of the signal beam is measured by a spectrum analyser (OceanOptics Inc. HR2000), and fitted to a Gaussian in order to determine its centre wavelength and spectral full width at half maximum. These are used to calculate the Raman shift being probed, the anti-Stokes wavelength, and the CARS spectral bandwidth.

Additional small fractions of the signal and idler beam are removed and their intensities measured by photodiodes. In the idler mode, the photomultiplier output signal obtained from the lock-in amplifier is divided by the product of the square of the current from the signal photodiode with the current from the idler photodiode; compare Eqn (1). In the fundamental mode, the Stokes intensity is constant and the idler is not used, so the current from the idler photodiode is ignored. The resulting output signal is then corrected for the photomultiplier sensitivity as a function of the anti-Stokes wavelength.

The CARS spectra thus obtained were smoothed with a central moving average filter 2.5 cm^{-1} wide, and then processed using the maximum entropy method of phase retrieval[10] in an online application kindly made available by the AMOLF institute of Amsterdam.[15]

Results and Discussion

The OPO emits tunable infrared light of 880–1040 nm (signal) and 1090–1350 nm (idler), limited at both ends of the range by the reflection coating on the cavity mirrors, which permits operation almost to the degeneracy point. This is similar to a commercial OPO (APE-Berlin) which has recently been extended to include continuous scanning; however, its maximum reachable signal wavelength of 990 nm is not as close to the degeneracy point
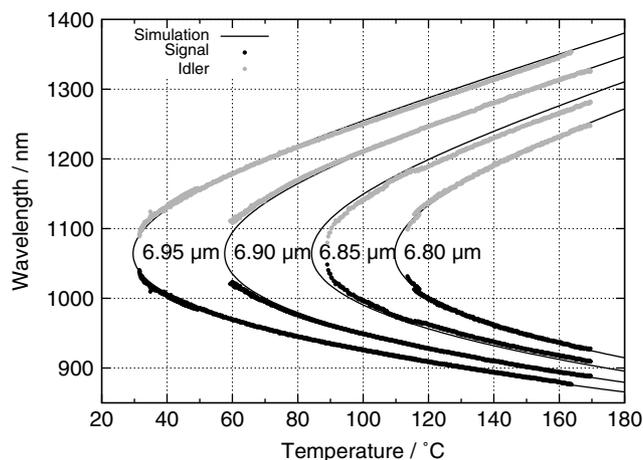

Figure 3. Temperature tuning curve of the OPO for four different poling periods of the MgO : PPLN crystal. The solid lines are calculated.

as the OPO described here; and it requires substantially more pumping power (and generates more output).

The average spectral full width at half maximum of the signal light is 26.0 cm^{-1}. When tested with the second pump laser, the average spectral width was much smaller, from 3 to 5 cm^{-1}, suggesting that the OPO is capable of producing spectrally narrower light for CARS measurements. However, the second pump laser was not available for CARS measurements.

Selecting a poling period in the MgO : PPLN crystal allows coarse tuning of the OPO's output wavelengths, while changing the crystal temperature allows fine tuning. The scanning speed is limited by the crystal's maximum heating/cooling rate of 10 °C min^{-1}. Figure 3 shows the temperature tuning curve for each of the four poling periods used, along with predictions according to a temperature-dependent Sellmeier equation for 5 mol% MgO : PPLN.[16] The signal wavelength was measured while changing the temperature, and the idler wavelength was calculated from the signal wavelength.

Fine tuning can be done to a certain extent without realigning the cavity. Depending on the quality of the cavity alignment, continuous scanning can be achieved for 12–18 nm to either side of the signal wavelength at which the cavity was aligned. After that, the cavity length must be adjusted to compensate for the changing optical path length of the crystal. Outside of this range, the spectral width of the signal broadens, or the OPO stops oscillating.

By tuning the wavelength of the signal, which is used as the pump/probe beam in the CARS process, the setup can address individual molecular vibrations from 436–3677 cm^{-1} (in idler mode) or 218–1838 cm^{-1} (in fundamental mode.) These correspond to anti-Stokes wavelengths of 670.6–994.9 nm and 764.9–1017.0 nm, respectively. In practice, the detection limit of the setup is an anti-Stokes wavelength of 890 nm or a Raman shift of 900 cm^{-1}, because the photomultiplier tube's sensitivity decreases exponentially at higher wavelengths.

To determine the effect of the variable output coupler on the OPO output, the signal and idler output powers were measured for various rotation angles of the half-wave plate. Figure 4 is a graph of these output powers, compared to rough predictions from a model based on continuous-wave Gaussian pump beams,[17] which is asserted to hold for pulsed Gaussian pump beams with a rectangular temporal pulse shape.[18]
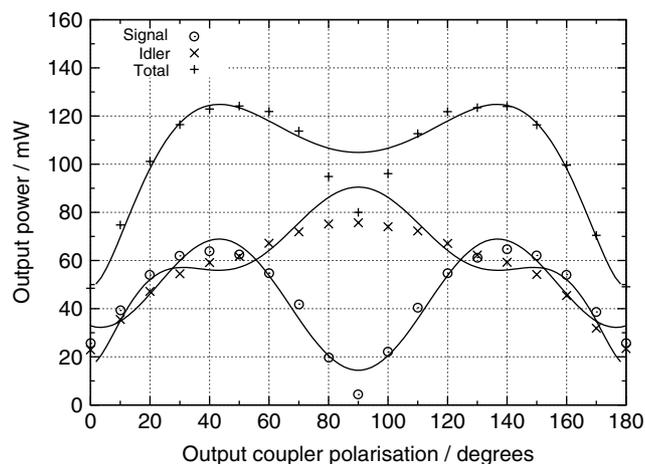
Copyright © 2009 John Wiley & Sons, Ltd.

www.interscience.wiley.com/journal/jrs

Figure 4. Signal and idler output power, and total power, as a function of the variable output coupler polariser angle. The solid lines are qualitative predictions from a model based on continuous-wave Gaussian pump beams.[17].
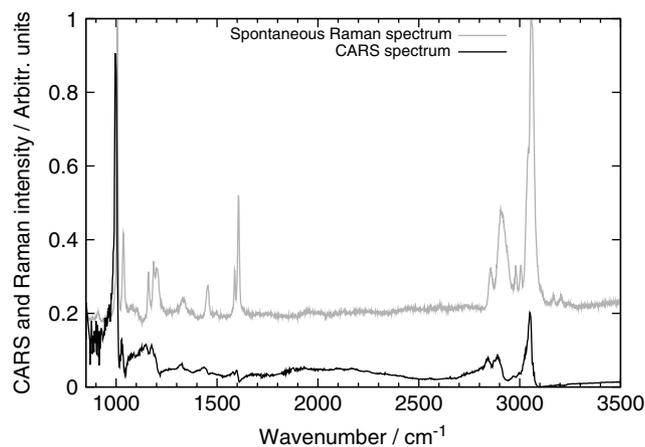

Figure 6. Comparison of the 1585 and 1603 cm^{-1} lines in polystyrene, in idler mode (calculated spectral resolution $\Delta \tilde{\nu} = 36.8$ cm^{-1}) and fundamental mode ($\Delta \tilde{\nu} = 26.0$ cm^{-1}). In the latter mode, the two neighbouring peaks are easily resolvable.

Figure 5. CARS spectrum of polystyrene. The spontaneous Raman spectrum is shown with an arbitrary offset from the CARS spectrum for clarity.

Figure 7. Raman lineshapes extracted from a CARS spectrum using the maximum entropy method[10,15]. The corresponding wavenumbers from spontaneous Raman data are indicated above the CARS peaks. The inset is an enlargement of part of the fingerprint region.

In the present CARS experiment, the output coupler is always set to maximum signal output. When attempting CARS using the idler and 1064 nm beams, it can be set to maximum idler output at 90°, since no signal power is coupled out of the cavity at that angle.

CARS spectra of several substances with well-known Raman spectra were recorded. A spectrum from 900 to 3600 cm^{-1} can be recorded in six scans, adjusting the OPO cavity length and realigning in between. The scanning speed depends on the poling period used: in this experiment, the 6.90 and 6.95 μm domains were used, which requires approximately 3 minutes for each scan; however, if the 6.80 μm domain were to be used, the OPO's entire range of output wavelengths could be covered in under 6 minutes.

Each scan is necessarily recorded with the alignment slightly different, causing variations in output power. These are corrected by overlapping the scan ranges and normalising accordingly when splicing them together.

As a demonstration of the technique, the spectrum of bulk polystyrene is shown in Fig. 5. The strong aromatic ring stretching vibration around 1000 cm^{-1} is clearly visible, as is the C–H stretching region from 2800–3100 cm^{-1}.
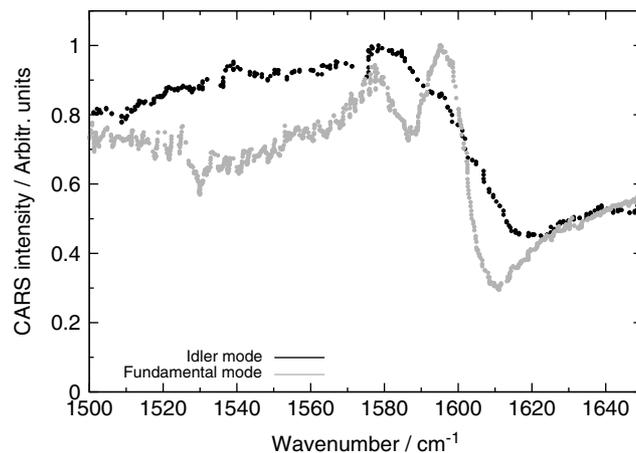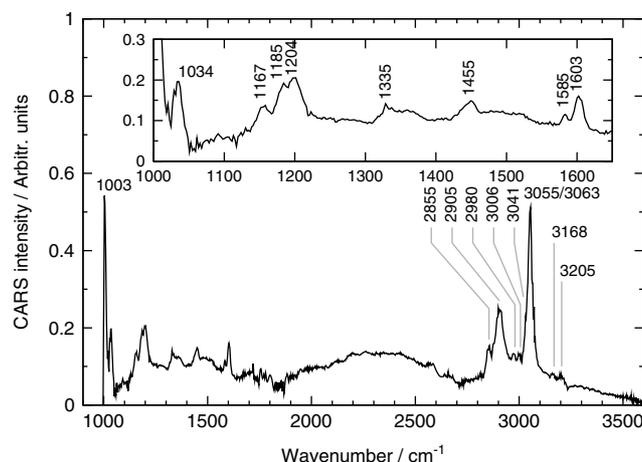
It is instructive to examine the effect of the pulse bandwidth on the spectral resolution. Equation (4) gives the CARS bandwidth in terms of the pulse bandwidths, with the 1064 nm pulse bandwidth being estimated from the laser's pulse length using the time-bandwidth product of a Gaussian pulse.

Figure 6 compares two measurements of the same region of polystyrene, recorded in idler mode and fundamental mode. The CARS bandwidths of the two modes were calculated using Eqn (4). The two neighbouring peaks at 1585 and 1603 cm^{-1} are clearly resolvable in fundamental mode with its narrower CARS bandwidth of 26.0 cm^{-1}, while the idler mode's broader bandwidth of 36.8 cm^{-1} decreases the spectral resolving power to the point where the two peaks overlap.

Figure 7 shows the results of applying the maximum entropy method to the CARS spectrum of polystyrene. Compared to Fig. 5, the lineshapes in the processed spectrum exhibit much more similarity to those in the spontaneous Raman spectrum, and are visible much more clearly. The resonances at 1585 and 1603 cm^{-1}

are far less intense in the processed spectrum. This can be ascribed to spectral broadening of the OPO outputs.

Correcting the CARS output data for the signal and idler intensity introduces extra sources of noise in addition to the noise already present, e.g. in the photomultiplier or the temperature fluctuations in the MgO : PPLN crystal. However, the signal-to-noise ratio is far more than sufficient for the CARS resonances to be clearly discernible in Figs. 5–7.

Conclusions and Outlook

In this work, we described and characterised a specially designed OPO used as a tunable source of coherent light for CARS spectroscopy. The OPO features a novel variable output coupler, allowing any desired fraction of the signal beam to be coupled out of the cavity. The OPO emits light of 880–1040 nm (signal) and 1090–1350 nm (idler), with a narrow bandwidth of 26.0 cm^{-1} on average.

We achieved high spectral resolution, continuous CARS spectroscopy from 900 to 3600 cm^{-1}, covering a large part of the fingerprint region, on polystyrene, a sample organic substance. Acquiring the CARS spectrum required only one detector.

We used the maximum entropy method of phase retrieval as a substitute for heterodyne interferometric detection to compare the measured CARS spectra to spontaneous Raman spectra, which were in extremely good agreement. We also examined the effects of input pulse spectral width on the CARS intensity and spectral resolution.

In a follow-up experiment, using a photomultiplier tube sensitive to at least 1050 nm would enable scanning to about 250 cm^{-1}, more than enough to cover the entire fingerprint region. This would also allow the 1064 nm light to be used as the CARS pump/probe light and the OPO's idler as the Stokes light. This CARS scheme would also allow heterodyne detection.[8]

Another possible future improvement is to reduce the pulse spectral width, which will improve the CARS spectral resolution and reduce the nonresonant background. The mechanism for adjusting the cavity length could also be motorised, which would considerably decrease the time necessary to acquire a full spectrum.

References

[1] J.-X. Cheng, X. S. Xie, *J. Phys. Chem. B* **2004**, *108*, 827.
[2] F. Ganikhanov, S. Carrasco, X. S. Xie, M. Katz, W. Seitz, D. Kopf, *Opt. Lett.* **2006**, *31*, 1292.
[3] R. W. Boyd, *Nonlinear Optics* (2nd edn), Academic Press: **2003**, 460p, 461p.
[4] A. Zumbusch, G. R. Holtom, X. S. Xie, *Phys. Rev. Lett.* **1999**, *82*, 4142.
[5] H. Lotem, R. T. Lynch Jr, N. Bloembergen, *Phys. Rev. A* **1976**, *14*, 1748.
[6] C. L. Evans, X. S. Xie, *Annu. Rev. Anal. Chem.* **2008**, *1*, 883.
[7] J.-X. Cheng, A. Volkmer, L. D. Book, X. S. Xie, *J. Phys. Chem. B* **2001**, *105*, 1277.
[8] M. Jurna, J. P. Korterik, C. Otto, J. L. Herek, H. L. Offerhaus, *Opt. Express* **2008**, *16*, 15863.
[9] E. O. Potma, C. L. Evans, X. S. Xie, *Opt. Lett.* **2006**, *31*, 241.
[10] E. M. Vartiainen, H. A. Rinia, M. Müller, M. Bonn, *Opt. Express* **2006**, *14*, 3622.
[11] M. J. McCarthy, D. C. Hanna, *Opt. Lett.* **1992**, *17*, 402.
[12] C. Otto, A. Voroshilov, S. G. Kruglik, J. Greve, *J. Raman Spectrosc.* **2001**, *32*, 495.
[13] A. Voroshilov, PhD. Thesis, *Polarised Coherent Raman and Saturation Micro-Raman Studies of Biological Macromolecules*. University of Twente (Enschede), **1997**.
[14] National Instruments, Inc. http://digital.ni.com/express.nsf/bycode/lockin [accessed: 2008].
[15] M. Bonn, E. M. Vartiainen, Online software application, http://memcars.amolf.nl [accessed: 2008].
[16] H. P. Li, D. Y. Tang, S. P. Ng, J. Kong, *Opt. Laser. Technol* **2006**, *38*, 192.
[17] J. Bjorkholm, *IEEE J. Quantum Electron.* **1971**, *7*, 109.
[18] T. W. Tukker, C. Otto, J. Greve, *J. Opt. Soc. Am. B* **1999**, *16*, 90.